PERGAMON

Journal of Structural Geology 23 (2001) 1337–1344

JOURNAL OF STRUCTURAL GEOLOGY

www.elsevier.com/locate/jstrugeo

# Effects of water on dynamically recrystallized grain-size of olivine

Haemyeong Jung, Shun-Ichiro Karato*

*Department of Geology and Geophysics, University of Minnesota, Minneapolis, MN 55455, USA*

Received 19 June 2000; revised 5 December 2000; accepted 21 December 2000

**Abstract**

Recrystallized grain-size versus stress relationship for olivine has been determined under water-poor and water-rich conditions. We found that when the water content in olivine exceeds ~800 ppm H/Si, the size of recrystallized grains is about two to three times larger than under water-poor conditions, compared at the same stress level. Microstructural observations of deformed samples show that the ratio of recrystallized grain size to that of subgrains increases significantly with water content and that the volume fraction of grains containing subgrain-boundaries is smaller under water-rich conditions than under water-poor conditions. These observations suggest that the enhancement of grain-boundary mobility by water is more significant than that of dislocation recovery, leading to a larger size of recrystallized grains under water-rich conditions. 

## 1. Introduction

The dynamically recrystallized grain-size versus stress relationship is a useful tool to infer the stress magnitude in naturally deformed rocks (Mercier et al., 1977; Nicolas, 1978; Karato et al., 1980; van der Wal et al., 1993). It is usually considered that the size of recrystallized grains is dependent only on stress and, therefore, the magnitude of stress can be inferred without knowing other variables such as temperature and water fugacity. However, the experimental study by Guillopé and Poirier (1979) and theoretical models by Guillopé and Poirier (1979), Derby and Ashby (1987) and Shimizu (1998) suggest that the size of recrystallized grains may depend also on other parameters that affect the kinetics of plastic deformation and grain-boundary migration. In particular, water content (or water fugacity) may affect grain-size because it has significant effects on plastic deformation (Mackwell et al., 1985; Karato, 1986; Karato et al., 1986) and on grain-boundary mobility (Karato, 1989). De Bresser et al. (1998) have recently demonstrated the temperature dependence of dynamically recrystallized grain size in hexagonal metals.

Some previous studies have addressed this issue and obtained conflicting results. Ross et al. (1980) argued that water significantly reduces the size of dynamically recrystallized grains of olivine. In contrast, van der Wal et al. (1993) investigated the effect of water content on dynamically recrystallized grain-size in olivine and were unable to detect any significant effects. We note, however, that there are several limitations in these previous studies. The earlier study by Ross et al. (1980) was made using a solid-medium deformation apparatus (the Griggs apparatus). Recent studies have demonstrated that the stress measurements using an outside load cell of the Griggs apparatus have very large uncertainties, exceeding 100% (e.g. Gleason and Tullis, 1993). Therefore, we consider that the results by Ross et al. (1980) are unreliable. Also, the study by van der Wal et al. (1993) has two limitations. First, the confining pressure used in that study is 300 MPa and, therefore, the solubility of water is only modest. At higher pressures, where the solubility of water in olivine is much higher (Kohlstedt et al., 1996), a more significant effect might be expected. Second, because of the presence of a significant amount of melt in the samples analyzed by van der Wal et al. (1993), water content in olivine is likely to be small due to a large partitioning of water into melt (Karato, 1987). Thus, we consider that the effects of water on dynamically recrystallized grain size in olivine have not been well understood by these previous studies.

In this study, we used modified experimental techniques to improve our understanding of the role of water on dynamically recrystallized grain-size in olivine. To realize high water fugacity conditions, we used a solid medium apparatus with a pressure medium that does not melt under the experimental conditions and measured water content in olivine using infrared spectroscopy. We also used a newly developed technique of stress estimation from dislocation density. This paper reports the results

* Corresponding author. Tel.: +1-612-624-1333, fax: +1-612-625-3819.
*E-mail address:* karato@tc.umn.edu (S.- Karato).

0191-8141/01/$ - see front matter 
PII: S0191-8141(01)00005-0

and discusses their implications for paleo-piezometers and other microstructural development in olivine.

## 2. Experimental technique

### 2.1. Starting materials and experimental procedures

We used both coarse-grained (~150 μm) natural dunite with a homogenous grain-size (from a kimberlite pipe at Jagersfontein, Southern Africa kindly supplied by S.E. Haggerty; for more details, see Jin (1995)) and olivine single crystals from San Carlos, Arizona. Single crystals of olivine were cut and oriented in a sample assembly to activate the (001)[100] slip system. Olivines in both samples have a composition of approximately Fa = 8% and Fo = 92%.

Deformation experiments were conducted using the Griggs apparatus at $P$ (pressure) = 2.0 GPa and $T$ (temperature) = 1473–1573 K using a simple shear sample assembly (e.g. Dell'Angelo and Tullis, 1989). Pressure was first raised to a desired value in ~5 h and then temperature was raised in ~1 h. After the temperature was stabilized, the piston was advanced at a constant rate using a stepping motor to provide a nearly constant strain-rate of deformation of a sample. Deformation experiments were conducted to ~60–400% strain. The pressure was kept constant and the uncertainties in the pressure estimate was less than ~10% (Mirwald et al., 1975). Temperature was measured using Pt/Rh thermocouples and the uncertainties in the temperature estimate was ~20 K, which were caused mostly by the temperature gradient through a sample. In 'wet' experiments, water was added to a sample by the decomposition of a talc plus brucite mixture (Fig. 1). We used brucite as well as talc to make sure that the material did not melt under experimental conditions. The talc plus brucite mixture was not in direct contact with the olivine specimen. The water (hydrogen) produced by dehydration reactions diffused through the nickel jacket and penetrated to the specimen. The amount of talc and brucite added was significantly larger than the amount to saturate a sample with water. In 'dry' experiments, no water was added and all parts were kept in an oven at ~473 K overnight to remove most of the adsorbed water.

After each experiment, the sample was first quenched to room temperature (within a few seconds) and pressure was reduced in 3–4 h. The water content of a sample was estimated from the infrared absorption spectroscopy on a quenched sample (single crystal olivine, water sensor, which is closed to the specimen) after each experiment using Nicolet 750 FT-IR spectrometer. We used the Paterson (1982) calibration to calculate the water content. Microstructures of a sample were observed by an optical microscope as well as by a scanning electron microscope (SEM). Sample strain was estimated from the rotation of a strain marker (Ni foil) that was inserted in a sample. The

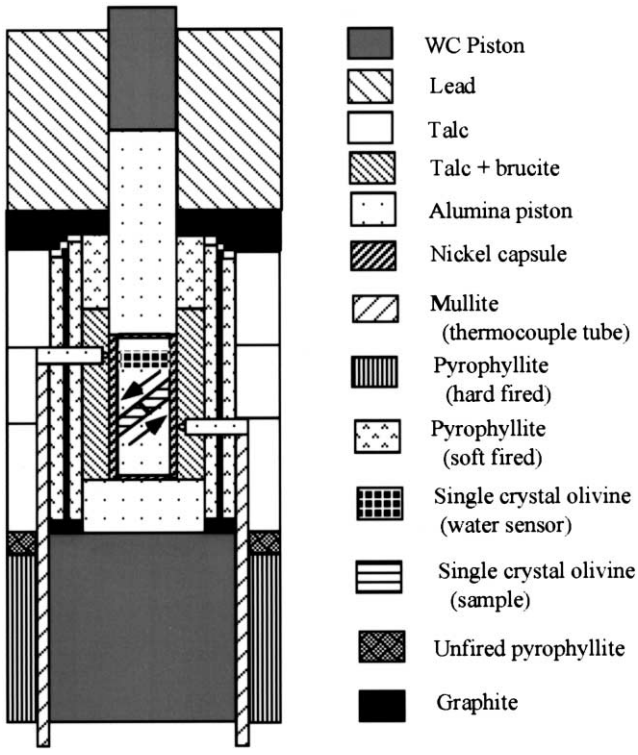


Fig. 1. A sample assembly for the shear deformation experiments. In 'wet' experiments, water was supplied by the dehydration of a mixture of talc and brucite. In 'dry' experiments, the mixture of talc and brucite was replaced with soft-fired pyrophyllite.

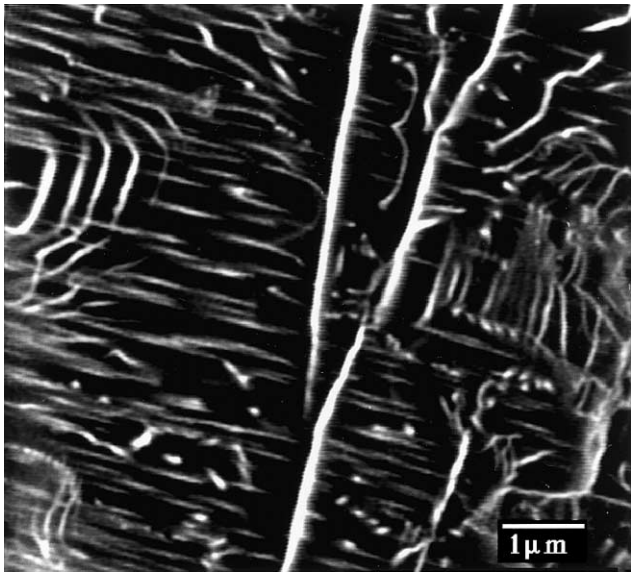


Fig. 2. A BEI of dislocations of a water-poor ('dry') sample, JK19. White lines are dislocations. The sample was decorated by oxidation in the air for 30 min at a temperature of 900°C. The BEI picture was taken at 15 kV acceleration voltage and 2 nA probe current.

Table 1
Deformation conditions and dislocation densities of samples used for calculation of dislocation density versus stress relationship (Fig. 3). All the experiments were conducted using a gas-medium apparatus. Stress was measured by an internal load cell. Starting materials are hot-pressed olivine aggregates. For the measurement of dislocation density, refer to the text

| Run | Pressure (MPa) | Temperature (K) | Dislocation density ($\times 10^{12}$/ $m^2$) | Stress (MPa) | Strain (%) |
|---|---|---|---|---|---|
| 4678 | 300 | 1573 | 0.90 | 112 | 7 |
| MIT-5 | 300 | 1573 | 1.81 | 200 | 11 |
| 284 | 300 | 1473 | 8.98 | 478 | 23 |

size of the recrystallized grains was measured by the intercept method using a scaling factor of 1.5 (Gifkins, 1970). About 500–1700 grains were measured in each sample.

### 2.2. Stress estimates

One of the most important technical issues in this study is the stress measurement. Usually, the differential stress acting on a sample in the Griggs apparatus is measured using a load cell located outside of the sample chamber. As a result, there is a significant contribution from friction to the load reading on a load cell (Gleason and Tullis, 1993). Green and his coworkers (Green and Borch, 1990; Tingle et al., 1993) improved this by introducing a liquid-cell sample assembly. With this assembly, the 'touch point' can be identified with higher resolution and hence the estimate of differential stress can also be made with higher resolution. The problems of friction cannot entirely be eliminated, however, and it becomes particularly serious when friction changes with strain.

Consequently, we used a new technique for stress estimation in this study. We used the free dislocation density ($\rho$) versus stress relationship to estimate the differential stress that acted on samples. The physical basis of such a relationship is the force balance between applied stress and the stress field around a dislocation (e.g. Poirier (1985)):

$$\rho = \alpha b^{-2}(\sigma/\mu)^2 \quad (1)$$

where $\alpha$ is a non-dimensional constant of order unity, $b$ is the length of the Burgers vector of dislocations, $\sigma$ is stress and $\mu$ is shear modulus. Material properties that come into play in such a relation are the shear modulus and the length of the Burgers vector. Because these properties do not change appreciably with water content or other physical–chemical parameters, we believe that such a relationship can reliably be used to estimate the stress magnitude in samples deformed under 'wet' as well as 'dry' conditions.

One complication is that such a relationship in a polycrystalline sample can be different from that for a single crystal. Presence of grain-boundaries could modify the dislocation density for several reasons. For example, 'geometrically necessary dislocations' caused by heterogeneous deformation near grain-boundaries could result in a higher dislocation density than single crystals (De Bresser, 1996). Fast grain-boundary migration may result in a lower dislocation density. Therefore, we constructed a new calibration curve for polycrystalline olivine using both the stress data that were obtained by a high-resolution gas apparatus (Karato et al., 1986; Zhang et al., 2000) and the measurements of dislocation density of each sample.

The measurement of dislocation density is a critical step. We used an oxidation decoration technique (Kohlstedt et al., 1976a) modified to SEM imaging (Karato, 1987) and measured dislocation density using a 'first principle' method, viz. (Karato and Lee, 1999):

$$\rho = \sum l/V \quad (2)$$

where $\sum l$ is the total length of dislocations in a volume $V$. The total length of dislocations is measured using NIH image-process software by measuring the total length of dislocation images (Fig. 2) captured by the back-scattered electron imaging (BEI) technique. The total length of dislocations was calculated from the measured length ($l_1$) on a SEM image through $l = \sqrt{l_1^2 + h^2}$ where $h$ is the effective thickness. The measurement was made at the acceleration

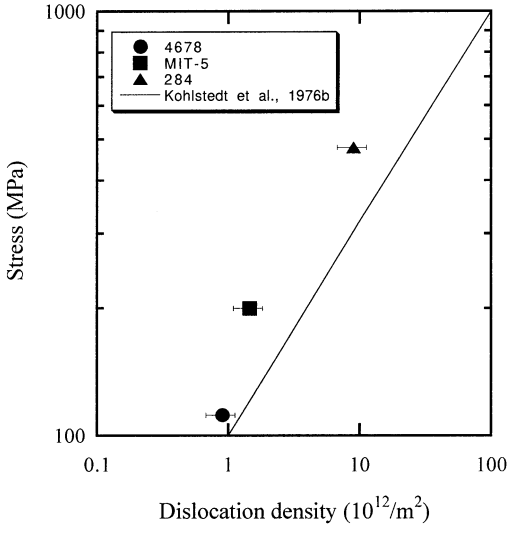


Fig. 3. Dislocation density versus stress relationship for samples deformed in a gas apparatus. Stresses in these samples were determined by an internal load cell (Table 2). The dislocation densities in these samples were determined by the BEI observations (for example, see Fig. 2). The solid line is the stress versus dislocation density relationship for a single crystal with the Schmid factor = 0.5 (Kohlstedt et al., 1976b).

Table 2
Experimental conditions and results. All the experiments were conducted at a pressure of 2 GPa using the Griggs apparatus

| Run no. | Water[a] | Starting material[b] | Temperature (K) | Time (min) | Shear strain (%) | Strain rate (1/s) | Dislocation density ($\times 10^{12}/m^2$) | Differential stress[c] (MPa) | Recrystallised grain size (μm) | Subgrain size (μm) |
|---|---|---|---|---|---|---|---|---|---|---|
| JK09 | Wet | Poly | 1473 | 21 | 100 | $7.9\times10^{-4}$ | 3.44 | 316 | 16.1 | 2.4 |
| JK10 | Wet | Poly | 1473 | 240 | 170 | $1.2\times10^{-4}$ | 1.67 | 198 | 27.6 | 2.6 |
| JK11 | Wet | Single | 1473 | 180 | 100 | $9.2\times10^{-5}$ | 2.05 | 231 | 31.4 | 3.5 |
| JK12 | Wet | Single | 1573 | 1518 | 100 | $6.9\times10^{-6}$ | 2.33 | 252 | 22.9 | 1.9 |
| JK18 | Wet | Single | 1473 | 21 | 120 | $9.5\times10^{-4}$ | 3.21 | 304 | 15.8 | – |
| JK19 | Dry | Single | 1573 | 324 | 120 | $1.7\times10^{-5}$ | 4.40 | 356 | 3.1 | 1.7 |
| JK21 | Dry | Single | 1573 | 366 | 400 | $7.9\times10^{-5}$ | 5.95 | 405 | 2.6 | 1.4 |
| JK25 | Damp[d] | Single | 1473 | 552 | 60 | $5.6\times10^{-6}$ | 2.98 | 292 | 8.4 | – |

[a] Wet: water-rich conditions (water content ≥ 800 ppm H/Si), dry: water-poor conditions (water content ≤ 200 ppm H/Si).
[b] Poly: natural dunite from a kimberlite pipe at Jagersfontein, Southern Africa, single: single crystal olivine from San Carlos, Arizona.
[c] Differential stress was measured from the dislocation density of the samples (see text for the detail).
[d] Water content of this sample was moderate (~450 ppm H/Si).

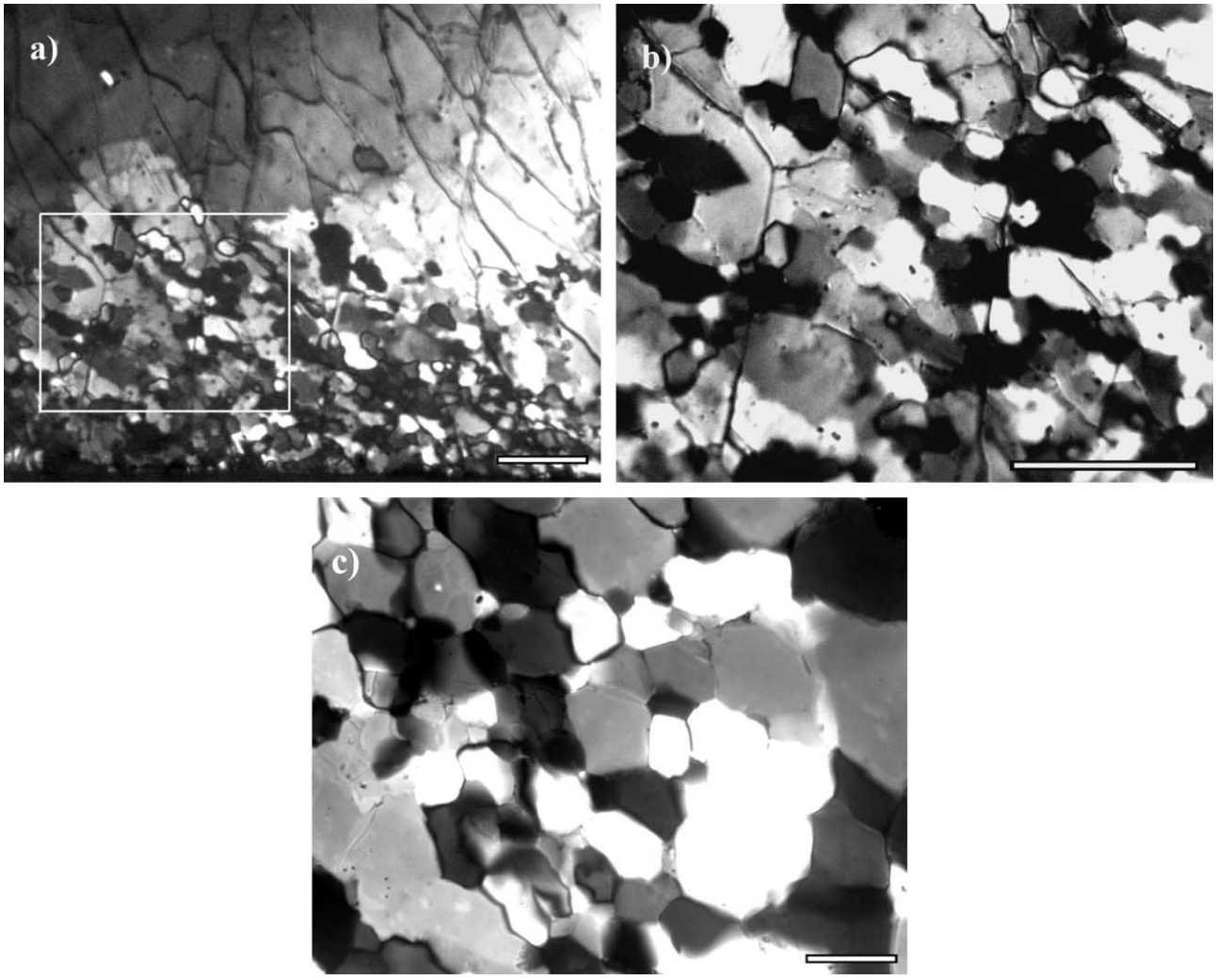


Fig. 4. Optical photomicrographs of deformed samples. Shear direction is top to the left for all the samples. (a) A sample (JK21) deformed under 'dry' conditions ($P = 2$ GPa, $T = 1573$ K. strain = 400%). The sample is only partially recrystallized. The bottom half of this picture corresponds to a recrystallized region. The top part remains as a single crystal containing subgrains with small misorientations. (b) An enlarged view of a rectangular region shown in (a). (c) A sample (JK18) deformed under 'wet' conditions ($P = 2$ GPa, $T = 1473$ K, strain = 120%). The sample is totally recrystallized. All the scale bars represent 20 μm.

voltage of 15 kV and the current of 2 nA. The effective thickness from which the dislocation image comes is calculated using a sample that contained nearly straight dislocations with known orientation: we oriented the sample surface such that dislocation lines are at 45° with respect to the surface and obtained dislocation images. From the length of dislocation images, we calculated the effective thickness from which dislocation images are obtained. The largest uncertainty in this technique is the error in the estimate of effective thickness which is ~10%.

Dislocation density in a polycrystalline aggregate is heterogeneous due to the distribution of crystallographic orientations, as well as the variation in local stresses caused by grain–grain interactions. Therefore, a statistical average was taken from the measurements of 30–50 grains in each sample. The total area from which dislocation density is determined for each sample is ~2000–3000 $\mu m^2$. The dislocation densities in each sample vary from grain to grain. The variation in dislocation density as measured by standard deviation is ~20–30%. The results are shown in Table 1 and Fig. 3, where we show the average dislocation densities with the standard deviations. The results follow Eq. (1). Therefore, the scatter of dislocation density measurements of ~20–30% can be translated into the uncertainty in stress estimate of ~10–15%. To estimate the stress of a sample, we used the new calibration based on the polycrystalline olivine data presented in this study.

## 3. Results

The experimental conditions and the results are summarized in Table 2. The experimental conditions may be

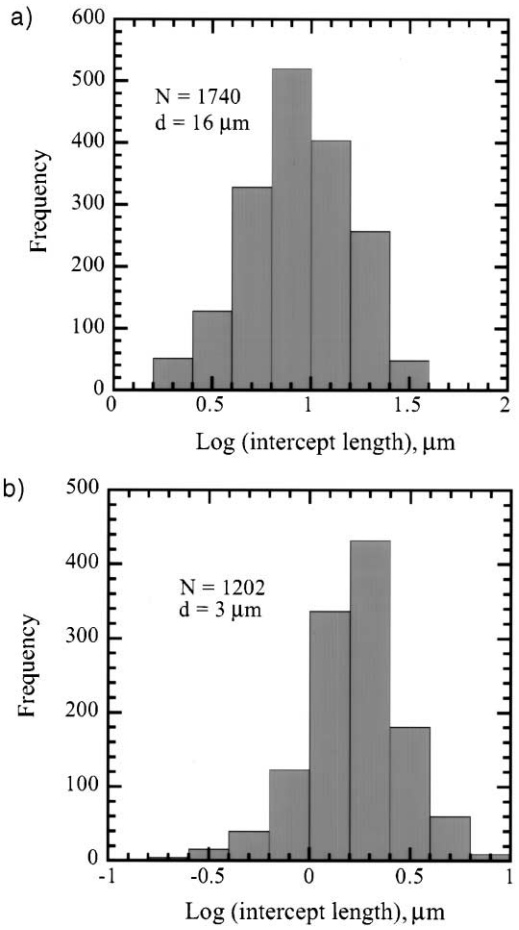


Fig. 5. Histograms of distribution of intercept lengths used for grain-size measurements for (a) JK18 ('wet') and (b) JK21 ('dry'). Both samples show nearly log-normal distribution but the 'dry' sample (JK21) shows wider grain-size distribution than the 'wet' one (JK18).

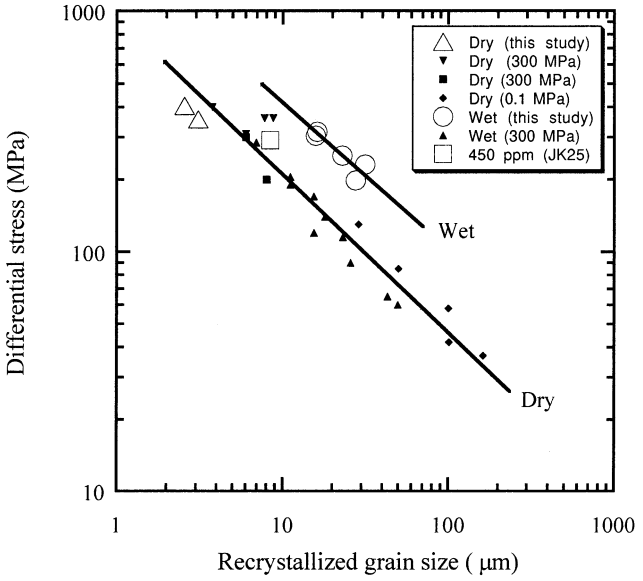


Fig. 6. Stress versus recrystallized grain-size relationship. Open symbols are from this work. Open circle: 'wet' condition, open triangle: 'dry' condition, open square: a sample with a moderate water content (JK25). Filled symbols are from the previous studies. Filled triangle: water-added but still dry condition at a pressure of 300 MPa with OH $<$ 200 ppm H/Si (van der Wal et al., 1993); filled inverse-triangle: dry condition (van der Wal et al., 1993); filled square: dry condition (Zhang et al., 2000); filled diamond: dry condition (Karato et al., 1980). Stress magnitudes in the samples from this study were estimated from dislocation densities. We used the linear intercept method to measure the grain size. All the data shown here were compared using the same correction factor ($C = 1.5$) for the 3D grain size. The solid lines indicate the results of the least square fit for the 'dry' and 'wet' condition. The size of recrystallized olivine deformed under 'wet' conditions is significantly larger than that under 'dry' conditions at the same stress.

divided into two categories: 'dry' (water-poor) and 'wet' (water-rich) conditions. The infrared spectroscopy observations for samples deformed under 'dry' (water-poor) conditions showed only a small amount of water, less than ~200 ppm H/Si. In most of the samples deformed under 'wet' (water-added) conditions, the infrared spectroscopy showed that the samples were saturated with water under the experimental conditions. In some cases (JK12, JK25), however, the amount of water in the samples was less than the solubility limit determined by Kohlstedt et al. (1996), suggesting some loss of water from these samples.

Optical micrographs of deformed samples are shown in Fig. 4. In 'wet' conditions, single crystals of olivine were totally recrystallized after ~100% shear strain (at $T = 1473$ K and $P = 2$ GPa). In contrast, in 'dry' conditions, the degree of recrystallization is more limited. Even at ~400% shear strain (at $T = 1573$ K and $P = 2$ GPa), the degree of recrystallization is only ~50%. It is also observed that subgrain development is more significant in 'dry' samples than 'wet' ones.

The grain-size distribution is nearly log-normal (Fig. 5) and we use the average grain-size as determined by the intercept method in this paper. Grain-size distribution in 'dry' samples is broader than in 'wet' samples. Average recrystallized grain-sizes for both 'dry' (water-poor) and 'wet' (water-rich) samples are plotted against stress in Fig. 6, along with some previous data (Karato et al., 1980; van der Wal et al., 1993; Zhang et al., 2000). The data in this study for 'dry' conditions are consistent with previous studies. The data for 'wet' conditions, however, show that recrystallized grain-size is at least two to three times larger than that of the previous studies, compared at the same stress. In more detail, this water effect on grain-size becomes appreciable when water content exceeds ~800 ppm H/Si (JK12): the grain-size of this sample is similar to those in samples that are saturated with water (water content ~1400 ppm H/Si). A sample that contains somewhat intermediate water content (~450 ppm H/Si; JK25) showed an intermediate grain-size.

## 4. Discussion

This study demonstrates that water has a strong influence

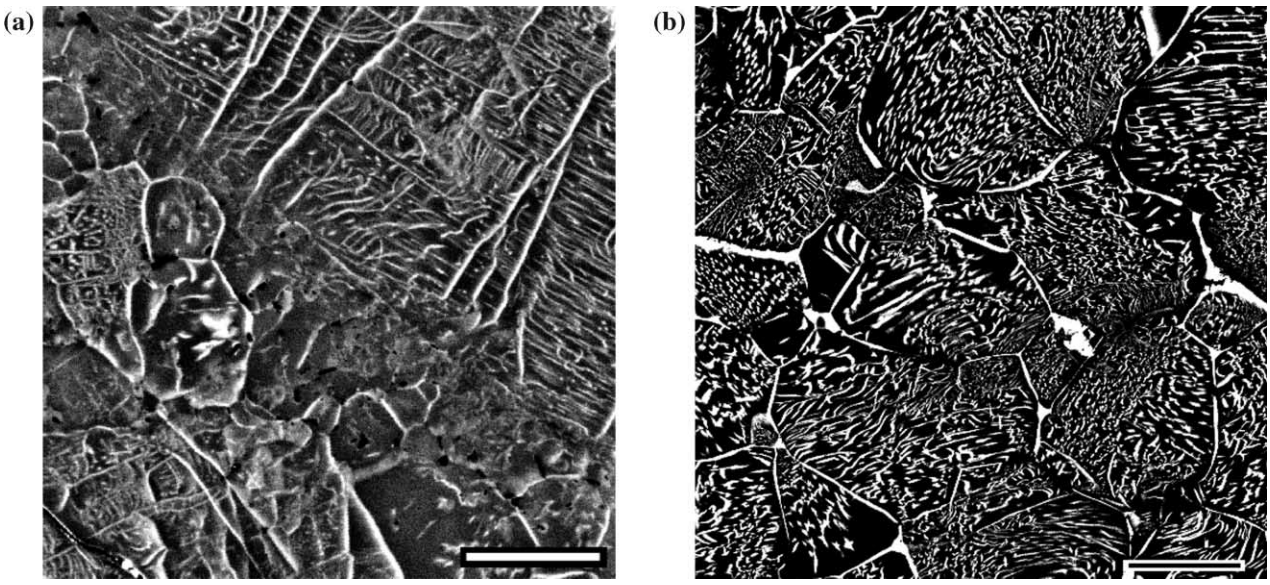


Fig. 7. Backscattered electron images of samples deformed (a) 'dry' (JK19) and (b) 'wet' (JK18) conditions. Note that the sample deformed under 'dry' conditions contains subgrain boundaries in a large fraction of grains, whereas the sample deformed under 'wet' conditions contains subgrain boundaries only in a small fraction of grains. Scale bar represents 4 μm for (a) and 10 μm for (b).

on the recrystallized grain-size of olivine. To explore possible causes for this effect, we have examined dislocation microstructures of recrystallized samples (Fig. 7). Dislocation structures are quite different between 'dry' and 'wet' samples (Fig. 7). In 'dry' samples, we observed well-developed subgrains in a large fraction of grains. In contrast, in 'wet' samples, subgrain boundaries are observed only in a small fraction of grains. This is a notable observation because it is well known that water enhances dislocation recovery and, hence, promotes formation of subgrains (e.g. Mackwell et al., 1985). Therefore, our observation suggests that grain-boundary migration under 'wet' conditions is so fast that not much strain is accumulated in each grain to develop subgrains. We thus infer that water enhances grain-boundary migration more than subgrain formation (recovery). This enhanced grain-boundary migration has a potential influence on the stress estimation from dislocation density. Due to the rapid migration of grain-boundaries, dislocation densities in 'wet' samples could be lower than the 'dry' counter-part for a given stress. Therefore, stress for 'wet' samples could be underestimated and the actual effects of water on recrystallized grain-size can be somewhat larger than those reported here.

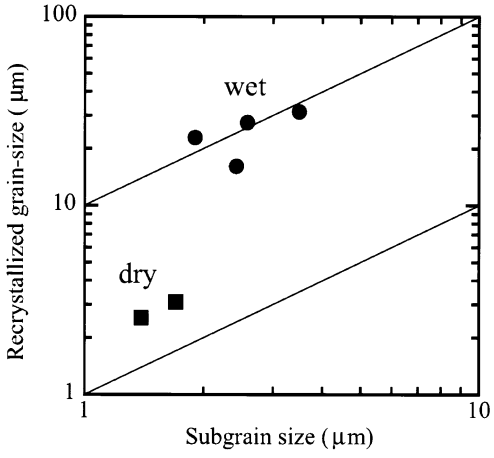


Fig. 8. Recrystallized grain-size versus subgrain size relationship. The recrystallized grain-size is a factor of ~2 larger than that of subgrain size under 'dry' conditions, whereas it is a factor of ~10 larger than subgrain-size under 'wet' conditions.

Another observation is the size of subgrains (subgrain spacing) relative to the size of recrystallized grains. Fig. 8 shows the plot of recrystallized grain-size against subgrain spacing. The ratio, [recrystallized grain-size]/[subgrain spacing], is ~2 for 'dry' conditions, whereas it is ~10 for 'wet' conditions. This again suggests significant enhancement of grain-boundary migration by water.

The enhancement of grain-boundary migration by water is likely to be a result of modification of grain-boundary structure and bonding. We noticed that grain-boundaries in 'wet' samples are much weaker than those in 'dry' ones: many grains plucked out very easily when we polished 'wet' samples. It appears that water reduces the strength of chemical bonding at grain-boundaries and enhances their mobility.

The above observation is consistent with a model by Guillopé and Poirier (1979) who proposed that the recrystallized grain-size versus stress relation may be dependent on the rate of grain-boundary migration. We suggest that the dominant process of dynamic recrystallization under 'dry' conditions is subgrain rotation (associated with a limited amount of grain-boundary migration) but the strain-induced grain-boundary migration plays a more important role under 'wet' conditions.

## 5. Conclusions

Our results have a direct influence on the stress estimates from recrystallized grain-size. Water has a strong influence on the recrystallized grain-size of olivine. The recrystallized grain-size is much larger under 'wet' conditions than that under 'dry' conditions. The critical amount of water that changes the recrystallized grain-size is ~800 ppm H/Si, which is below the estimated water content in the asthenosphere (e.g. Hirth and Kohlstedt, 1996; Karato and Jung, 1998). Therefore, the inference of stress magnitude from the recrystallized grain-size of olivine needs to be reconsidered when applied to samples that have been deformed under 'wet' conditions. We also infer that water enhances grain-boundary migration relative to subgrain rotation (recovery) and changes the dominant process of dynamic recrystallization from subgrain rotation (under 'dry' conditions) to grain-boundary migration under 'wet' conditions. Enhanced grain-boundary migration by water may affect other processes, including lattice preferred orientation.

## Acknowledgements

This research was supported by grants from NSF (EAR-9903087, EAR-9906986). H. Jung gives thanks for financial support through the Doctoral Dissertation Fellowship from the University of Minnesota. We thank K.-H. Lee for his help in electron microscopy at the beginning of this research and S. Mei for discussion.

## References

De Bresser, J.H.P., 1996. Steady state dislocation densities in experimentally deformed calcite materials: single crystals versus polycrystals. Journal of Geophysical Research 101, 22189–22202.

De Bresser, J.H.P., Peach, C.J., Reijs, J.P.J., Spiers, C.J., 1998. Geophysical Research Letters 25, 3457–3460.

Dell'Angelo, L.N., Tullis, J., 1989. Fabric development in experimentally sheared quartzites. Tectonophysics 169, 1–21.

Derby, B., Ashby, M.F., 1987. On dynamic recrystallization. Scripta Metallurgica 21, 879–884.

Gifkins, R.C., 1970. Optical Microscopy of Metals. Elsevier, New York.

Gleason, G.C., Tullis, J., 1993. Improving flow laws and piezometers for quartz and feldspar aggregates. Geophysical Research Letters 20, 2111–2114.

Green, H.W., Borch, R.S., 1990. High pressure and temperature deformation experiments in a liquid confining medium. Geophysical Monograph 56, 195–200.

Guillopé, M., Poirier, J.-P., 1979. Dynamic recrystallization during creep of single-crystalline halite: an experimental study. Journal of Geophysical Research 84, 5557–5567.

Hirth, G., Kohlstedt, D.L., 1996. Water in the oceanic upper mantle: implications for rheology, melt extraction and the evolution of the lithosphere. Earth and Planetary Science Letters 144, 93–108.

Jin, D., 1995. Deformation microstructures of some ultramafic rocks. M.S. Thesis, University of Minnesota.

Karato, S., 1986. Does partial melting reduce the creep strength of the upper mantle? Nature 319, 309–310.

Karato, S., 1987. Scanning electron microscope observation of dislocations in olivine. Physics and Chemistry of Minerals 14, 245–248.

Karato, S., 1989. Grain growth kinetics in olivine aggregates. Tectonophysics 168, 255–273.

Karato, S., Jung, H., 1998. Water, partial melting and the origin of the seismic low velocity and high attenuation zone in the upper mantle. Earth and Planetary Science Letters 157, 193–207.

Karato, S., Lee, K.-H., 1999. Stress-strain distribution in deformed olivine aggregates: Inference from microstructural observations and implications for texture development. In: Szpunar, J.A. (Ed.) Proceedings of the Twelfth International Conference on Textures of Materials. ITOCOM-12, Vol. 2. , pp. 1546–1555.

Karato, S., Toriumi, M., Fujii, T., 1980. Dynamic recrystallization of olivine single crystals during high-temperature creep. Geophysical Research Letters 7, 649–652.

Karato, S., Paterson, M.S., Fitz Gerald, J.D., 1986. Rheology of synthetic olivine aggregates: influence of grain size and water. Journal of Geophysical Research 91, 8151–8176.

Kohlstedt, D.L., Goetze, C., Durham, W.B., Vander Sande, J.B., 1976a. New technique for decorating dislocations in olivine. Science 191, 1045–1046.

Kohlstedt, D.L., Goetze, C., Durham, W.B., 1976b. Experimental deformation of single crystal olivine with application to flow in the mantle. In: Strens, R.G.J. (Ed.). The Physics and Chemistry of Minerals and Rocks. John Wiley & Sons, pp. 35–49.

Mackwell, S.J., Kohlstedt, D.L., Paterson, M.S., 1985. Role of water in the deformation of olivine single crystals. Journal of Geophysical Research 90, 11319–11333.

Mercier, J.-C.C., Anderson, D.A., Carter, N.C., 1977. Stress in the lithosphere: inferences from steady state flow of rocks. Pure and Applied Geophysics 115, 199–226.

Mirwald, P.W., Getting, I.C., Kennedy, G.C., 1975. Low-friction cell for piston-cylinder high-pressure apparatus. Journal of Geophysical Research 80, 1519–1525.

Nicolas, A., 1978. Stress estimates from structural studies in some mantle peridotites. Philosophical Transaction of the Royal Society of London Ser. A. 288, 49–57.

Paterson, M.S., 1982. The determination of hydroxyl by infrared absorption in quartz, silicate glasses and similar materials. Bulletin of Mineralogy 105, 20–29.

Poirier, J.P., 1985. Creep of Crystals. Cambridge Unversity Press, Cambridge, pp. 260.

Ross, J.V., AveLallemant, H.G., Carter, N.L., 1980. Stress dependence of recrystallized-grain size and subgrain size in olivine. Tectonophysics 70, 39–61.

Shimizu, I., 1998. Stress and temperature dependence of recrystallized grain size: a subgrain misorientation model. Geophysical Research Letters 25, 4237–4240.

Tingle, T.N., Green, H.W., Young, T.E., 1993. Improvements to Griggs-type apparatus for mechanical testing at high pressures and temperatures. Pure and Applied Geophysics 141, 523–543.

van der Wal, D., Chopra, P., Drury, M., Fitz Gerald, J., 1993. Relationships between dynamically recrystallized grain size and deformation conditions in experimentally deformed olivine rocks. Geophysical Research Letters 20, 1479–1482.

Zhang, S., Karato, S., Fitz Gerald, J.D., Faul, U.H., Zhou, Y., 2000. Simple shear deformation of olivine aggregates. Tectonophysics 316, 133–152.